Article

Local Environments and Lithium Adsorption on the Iron Oxyhydroxides Lepidocrocite (□-FeOOH) and Goethite (□-FeOOH): A H and Li Solid-State MAS NMR Study

Jongsik Kim, Ulla Gro Nielsen, and Clare P. Grey

J. Am. Chem. Soc., **2008**, 130 (4), 1285-1295 • DOI: 10.1021/ja0761028

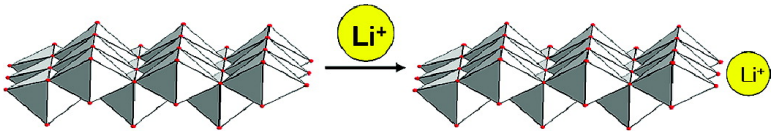

More About This Article

J|A|C|S
ARTICLES
Published on Web 01/09/2008

Local Environments and Lithium Adsorption on the Iron Oxyhydroxides Lepidocrocite (γ-FeOOH) and Goethite (α-FeOOH): A ^{2}H and ^{7}Li Solid-State MAS NMR Study

Jongsik Kim,[†,‡] Ulla Gro Nielsen,[†,‡] and Clare P. Grey*[,†,‡]

Center for Environmental Molecular Science (CEMS), and Department of Chemistry, Stony Brook University, Stony Brook, New York 11794-3400

Received August 13, 2007; E-mail: cgrey@notes.cc.sunysb.edu

Abstract: ^{2}H and ^{7}Li MAS NMR spectroscopy techniques were applied to study the local surface and bulk environments of iron oxyhydroxide lepidocrocite (γ-FeOOH). ^{2}H variable-temperature (VT) MAS NMR experiments were performed, showing the presence of short-range, strong antiferromagnetic correlations, even at temperatures above the Néel temperature, T_N, 77 K. The formation of a Li^+ inner-sphere complex on the surface of lepidocrocite was confirmed by the observation of a signal with a large ^{7}Li hyperfine shift in the ^{7}Li MAS NMR spectrum. The effect of pH and relative humidity (RH) on the concentrations of Li^+ inner- and outer-sphere complexes was then explored, the concentration of the inner sphere complex increasing rapidly above the point of zero charge and with decreasing RH. Possible local environments of the adsorbed Li^+ were identified by comparison with other layer-structured iron oxides such as γ-$LiFeO_2$ and *o*-$LiFeO_2$. Li^+ positions of Li^+-sorbed and exchanged goethite were reanalyzed on the basis of the correlations between Li hyperfine shifts and Li local structures, and two different binding sites were proposed, the second binding site only becoming available at higher pH.

1. Introduction

Over the past decade, iron oxides and hydroxides have been studied as effective sorbents to remove toxic materials from polluted water and nuclear waste streams due to their high surface areas and affinities for metal ions.[1−5] In addition, the interactions between iron oxides and hydroxides and metals influence the fate, and in particular the mobility, of metals in groundwater. Hence, an understanding of the molecular level mechanisms for adsorption of metals on soil minerals is important in order to predict the destiny of the adsorbed metal ions. The detection of changes in the uptake of small cations such as Li^+, Na^+, and Ag^+ on iron and manganese minerals can also be exploited to design sensors for these ions.[6,7] The mechanisms by which these systems function is not always clear, and methods to determine the modes of cation binding to these systems are required in order to characterize these systems more fully. There have been many studies which used spectroscopic techniques such as IR and X-ray absorption spectroscopy to determine the molecular basis for adsorption of various metal ions on iron-containing minerals.[8−16] However, very few solid-state NMR studies have been reported for these systems, due to the difficulties often associated with the investigation of paramagnetic (Fe^{3+}-containing) materials via this method.[17,18]

We recently reported a ^{2}H and ^{6}Li MAS NMR study of Li^+-sorbed and deuterated goethite (α-FeOOH).[17,18] The Néel temperature, T_N, of goethite is above 120 °C, and it is therefore antiferromagnetically ordered at room temperature. As a result, the ^{2}H MAS NMR spectrum of deuterated goethite was featureless and broad at room temperature, but well-resolved ^{2}H NMR spectra could be obtained by acquiring the data above T_N. Similarly, well-resolved spectra could also be obtained at ambient temperatures by either doping the material with Al^{3+} or by synthesizing nanoparticles, both methods leading to a reduction of T_N and to paramagnetic materials at room temper-

[†] Center for Environmental Molecular Science (CEMS).
[‡] Department of Chemistry.

(1) Deliyanni, E. A.; Bakoyannakis, D. N.; Zouboulis, A. I.; Matis, K. A. *Chemosphere* **2003**, *50*, 155−163.
(2) Ebner, A. D.; Ritter, J. A.; Navratil, J. D. *Ind. Eng. Chem. Res.* **2001**, *40*, 1615−1623.
(3) Marmier, N.; Delisee, A.; Fromage, F. *J. Colloid Interface Sci.* **1999**, *211*, 54−60.
(4) Cornell, R. M.; Schwertmann, U. *The Iron Oxides*; VCH: New York, 1996.
(5) Yavuz, C. T.; Mayo, J. T.; Yu, W. W.; Prakash, A.; Falkner, J. C.; Yean, S.; Cong, L.; Shipley, H. J.; Kan, A.; Tomson, M.; Natelson, D.; Colvin, V. L. *Science* **2006**, *314*, 964−967.
(6) Kanoh, H.; Feng, Q.; Miyai, Y.; Ooi, K. *J. Electrochem. Soc.* **1993**, *140*, 3162−3166.
(7) Poul, N. L.; Baudrin, E.; Morcrette, M.; Gwizdala, S.; Masquelier, C.; Tarascon, J.-M. *Solid State Ionics* **2003**, *159*, 149−158.
(8) Farquhar, M. L.; Charnock, J. M.; Livens, F. R.; Vaughan, D. J. *Environ. Sci. Technol.* **2002**, *36*, 1757−1762.
(9) Hsia, T. H.; Lo, S. L.; Lin, C. F.; Lee, D. Y. *Chemosphere* **1993**, *26*, 1897−1904.
(10) Leuz, A. K.; Monch, H.; Johnson, C. A. *Environ. Sci. Technol.* **2006**, *40*, 7277−7282.
(11) Mallikarjuna, N. N.; Venkataraman, A. *Talanta* **2003**, *60*, 139−147.
(12) Manceau, A.; Nagy, K. L.; Spadini, L.; Ragnarsdottir, K. V. *J. Colloid Interface Sci.* **2000**, *228*, 306−316.
(13) Peacock, C. L.; Sherman, D. M. *Geochim. Cosmochim. Acta* **2004**, *68*, 2623−2637.
(14) Peak, D.; Sparks, D. L. *Environ. Sci. Technol.* **2002**, *36*, 1460−1466.
(15) Randall, S. R.; Sherman, D. M.; Ragnarsdottir, K. V. *Geochim. Cosmochim. Acta* **2001**, *65*, 1015−1023.
(16) Gossuin, Y.; Colet, J.-M.; Roch, A.; Muller, R. N.; Gillis, P. *J. Magn. Reson.* **2002**, *157*, 132−136.
(17) Cole, K. E.; Paik, Y.; Reeder, R. J.; Schoonen, M.; Grey, C. P. *J. Phys. Chem. B* **2004**, *108*, 6938−6940.
(18) Nielsen, U. G.; Paik, Y.; Julmis, K.; Schoonen, M. A. A.; Reeder, R. J.; Grey, C. P. *J. Phys. Chem. B* **2005**, *109*, 18310−18315.

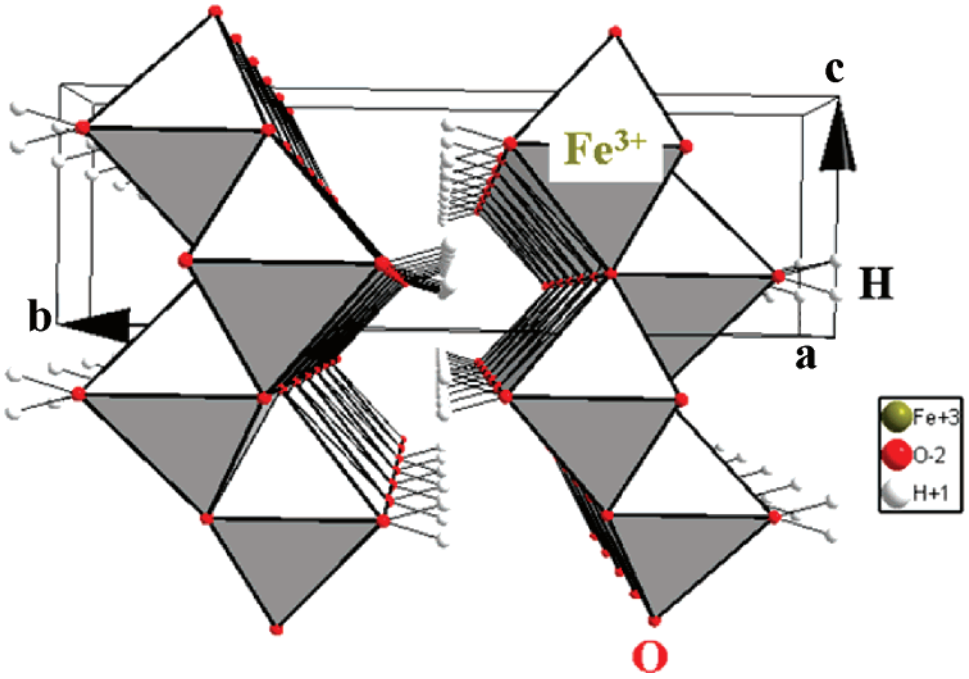

Figure 1. The crystal structure of lepidocrocite (γ-FeOOH) drawn with the reported crystallographic parameters.[20] Hydrogen atoms are on split positions.

ature. In contrast, the mineral lepidocrocite has a much lower T_N of 77 K, and so in principle, it should be straightforward to investigate this material even at room temperature. Thus, NMR studies can be performed under experimental conditions that are closer to those found in real adsorption systems. In addition, typical lepidocrocite samples have large surface areas of 15 to 260 m^2/g.[19] We therefore chose lepidocrocite as our model compound for sorption studies.

Lepidocrocite (γ-FeOOH) represents the second most prevalent iron oxyhydroxide in the soil and is typically formed under anerobic conditions.[4] Its unit cell is orthorhombic (space group *Cmcm*, $Z = 4$) with unit cell parameters $a = 3.072(2)$ Å, $b = 12.516(3)$ Å, $c = 3.873(2)$ Å (Figure 1).[20] The mineral is isostructural with boehmite (γ-AlOOH) and is comprised of a cubic close-packed array of O^{2-}/OH^- ions, the Fe^{3+} ordering to form zigzag sheets of Fe-octahedra, each layer being held together by hydrogen bonds. The zigzag sheets consist of double chains of Fe $(O, OH)_6$ octahedra which run parallel to the *c*-axis. The double chains share edges with adjacent double chains, where each chain is displaced by an octahedral unit with respect to its neighbor, forming the corrugated sheets of octahedra. These sheets are stacked perpendicular to the (010) direction and are separated by double rows of empty octahedral sites.[4] The predominant crystal plane of lepidocrocite is the (010) face, which contains doubly coordinated ($Fe^{3+}-O^{2-}-Fe^{3+}$) oxygen ions, and which typically accounts for 84% of the total surface area.[21] The protons can be replaced by Li^+ ions via an ion-exchange reaction, the Li^+ ions occupying the vacant octahedral sites between the corrugated layers to form *o*-$LiFeO_2$ (the "*o*"-indicating that this is the orthorhombic form of $LiFeO_2$).[22,23]

In this study, ^2H and ^7Li MAS NMR spectroscopy was used to probe the local bulk and surface environments of deuterated and lithiated lepidocrocite (γ-FeOOH). ^2H MAS NMR is an ideal method to characterize hydroxyl groups as the ^2H NMR line shape is very sensitive to the dynamics of the hydroxyl groups.[24] Moreover, ^2H has a lower gyromagnetic ratio than ^1H, resulting in a reduced dipolar interaction between the nuclear spins and magnetic moments due to the unpaired electrons of the Fe^{3+} ions. ^7Li MAS NMR is also a sensitive technique with which to study the lithium adsorption sites and pH and relative humidity effects on the Li binding. Li^+ was chosen as a model ion with which to study sorption, since we and others have reported the $^{6,7}Li$ MAS NMR spectra of various lithium-containing paramagnetic materials.[18,25] Large ^7Li hyperfine shifts were observed, which could be related to both the Li local environments (e.g., the number and bond angles of the $M-O-Li^+$ connectivities), and the number of unpaired electrons in the e_g and t_{2g} orbitals of the transition metal (M^{n+}) ions. Li^+ NMR spectroscopy should also represent a reasonable method for identifying and quantifying the strongest sorption sites that are also likely to bind small, ionic cations such as Na^+ and Mg^{2+}. We believe that this work should also serve as a good benchmark study allowing us to develop NMR approaches for investigating sorption on Fe^{3+}-containing systems, which should then be extendable to other NMR-active ionic ions such as Na^+ and Cs^+ and to more toxic cations such as Cd^{2+}, Pb^{2+}, etc.

This contribution reports results for Li^+sorption both as a function of pH and as a function of different relative humidities. The results are compared with ^7Li NMR spectra of Li^+-exchanged lepidocrocite, *o*-$LiFeO_2$,[23] in order to distinguish between surface and bulk sorption sites and to help establish correlations between Li hyperfine shifts and Li local environments. NMR spectra of lepidocrocite were compared with the previously reported spectra of goethite,[18] allowing potential sites for binding on these materials to be identified.

(19) Schwertmann, U.; Cornell, R. M. *Iron Oxides in the Laboratory*; VCH: New York, 1991.
(20) Zhukhlistov, A. P. *Crystallogr. Rep.* **2001**, *46*, 730−733.
(21) Ishikawa, T.; Nitta, S.; Kondo, S. *J. Chem. Soc., Faraday Trans. 1* **1986**, *82*, 2401−2410.
(22) Kanno, R.; Shirane, T.; Kawamoto, Y. *J. Electrochem. Soc.* **1996**, *143*, 2435−2442.
(23) Sakurai, Y.; Arai, H.; Okada, S.; Yamaki, J. *J. Power Sources* **1997**, *68*, 711−715.
(24) Duer, M. J. *Introduction to Solid-State NMR Spectroscopy*. Blackwell: 2004.
(25) Grey, C. P.; Dupre, N. *Chem. Rev.* **2004**, *104*, 4493−4512.

2. Experimental Section

2.1. Sample Preparation. 2.1.1. Deuterated Lepidocrocite. Lepidocrocite from Alfa Aesar, was suspended for one week in D_2O (98%, Cambridge Isotope Laboratories) to prepare deuterated lepidocrocite. The suspended lepidocrocite solution was shaken often. It was centrifuged and freeze-dried.[26]

2.1.2. Li^+ Adsorbed Lepidocrocite. Lepidocrocite (0.3 g) (Alfa Aesar) was suspended in 100 mL distilled water; 100 mL of a 50 mM $^7LiOH{\cdot}H_2O$ (Aldrich) solution was added to the suspension. The pH was then controlled by adding appropriate quantities of either a 1 M HNO_3 or 1 M NaOH solution to prepare three different suspensions at pH 4.0, 8.1 and 11.4, where the pH was measured by a OAKTON 2100 series pH meter with an OAKTON glass electrode. The pH values were chosen on the basis of our measured point of zero charge (PZC), pH 7.1, for our lepidocrocite sample. The solution was stirred for a day, and the Li-sorbed samples were then separated by centrifugation (5000 rpm) and dried in air. The pH 11.4 sample was subdivided, and the different parts were stored under different relative humidities of 30% and 84% for 1 day. The relative humidity was controlled by using saturated solutions of calcium chloride ($CaCl_2$) and potassium chloride (KCl), correspondingly.

A sample with a much lower Li^+ loading level was prepared by adding 100 mL of a 10 mM $^7LiOH{\cdot}H_2O$ solution to the 0.3 g lepidocrocite suspension. The same procedures used to synthesize the sample prepared at pH 11.4 were then followed. A pH 11.4 sample was also prepared as a wet paste by using the same method as used for the pH 11.4 sample, but without the drying procedure. Just before the NMR experiment, excess water was removed by pressing the sample between two pieces of filter paper.

2.1.3. Li^+ Intercalated Lepidocrocite (*o*-$LiFeO_2$). Lepidocrocite (0.3 g) (Alfa Aesar) was added to the solution of 2-phenoxyethanol (Aldrich) and lithium hydroxide (monohydrate) ($LiOH{\cdot}H_2O$, Aldrich). Li/Fe =1 in molar ratio was used. The solution was magnetically stirred and heated to 135 °C for 4 h, as described previously.[23] The Li^+ for H^+ ion-exchanged product was filtered and washed with ethanol several times and then dried under vacuum at 90 °C.

2.2. Characterization. 2.2.1. X-ray Diffraction (XRD) and Scanning Electron Microscopy (SEM). XRD data were collected for all samples on a Scintag powder X-ray diffractometer (Cu Kα radiation). All the diffraction patterns were compared with those in the Joint Committee on Powder Diffraction Standards (JCPDS). SEM images were obtained on a Leo 1550.

2.2.2. PZC (Point of Zero Charge) and BET (Brunauer, Emmett, and Teller) Surface Area. The particle size distribution and point of zero charge (PZC) were obtained by using a ZetaPlus (Brookhaven Instruments Corporation) for the protonated lepidocrocite sample. No attempt was made to remove the dissolved CO_2 from the solution. The BET surface area for the lepidocrocite sample was measured on a Micromeritics ASAP 2010 gas sorption analyzer using N_2.

2.2.3. Thermogravimetric Analysis (TGA) and Differential Thermal Analysis (DTA). TGA and DTA experiments were performed with a Netzsch (Germany), STA (simultaneous thermal analysis) 449 Jupiter instrument. The temperature was increased at a rate of 10 °C/min under an atmosphere of flowing nitrogen N_2. Weight loss was examined at temperatures ranging from ambient to 1050 °C.

2.2.4. Magic Angle Spinning (MAS) NMR. ^2H MAS NMR experiments were performed on CMX-200 and an INFINITY-360 spectrometers using a 1.8 mm Samoson probe and a 34 kHz spinning frequency (CMX-200) and a Chemagnetics 4 mm MAS probe with a 14 kHz spinning frequency (INFINITY-360). A rotor-synchronized, spin−echo pulse sequence was used with a pulse delay of 0.15 s, and the ^2H NMR spectra were referenced to D_2O at 4.8 ppm. Variable temperature (VT) experiments were performed from −75 to 150 °C.

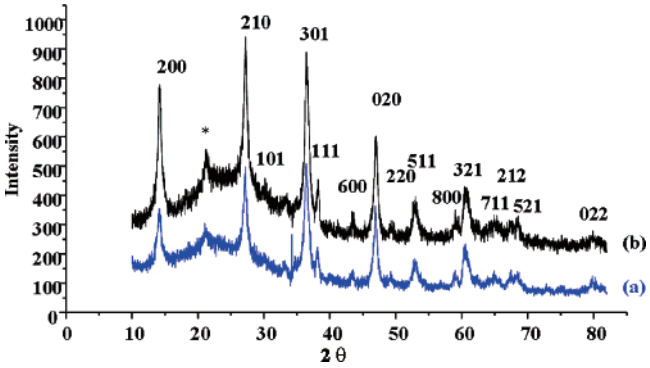

Figure 2. X-ray powder diffraction for (a) γ-FeOOH and (b) γ-FeOOD. (*) denotes the reflection due to the goethite impurity. The broad feature observed at around 15−30° is due to the quartz glass sample holder. Lepidocrocite peaks were indexed by using JCPDS.

^7Li solid-state NMR was performed on the CMX-200 and INFINITY-360 spectrometers. Chemagnetics 3.2 mm and Samoson 1.8 mm MAS probes were used on the CMX-200 spectrometer with 20 and 37 kHz spinning speeds, respectively. Chemagnetics 3.2 mm and 4 mm MAS probes were used on the INFINITY-360 spectrometer with a 15 kHz spinning speed. A rotor synchronized spin−echo pulse sequence was employed with an evolution period of one rotor period in the NMR experiments. The ^7Li NMR spectra were referenced to a 1.0 M ^7LiCl solution at 0 ppm. Spin−lattice relaxation (T_1) times were measured by using an inversion−recovery pulse sequence. Spin-counting experiments were performed to estimate the Li^+ surface coverage, by comparing the absolute intensity of the signals from the lepidocrocite samples with that from solid Li_2CO_3. The absolute intensities were measured by integrating the isotropic peaks and their respective spinning sidebands for data collected with the Chemagnetics 3.2 mm on the INFINITY-360 spectrometer. For Li^+-sorbed lepidocrocite, only the hyperfine-shifted resonances and their spinning side bands were considered. The intensities were normalized by the sample masses and the number of scans. For solid Li_2CO_3, a pulse delay of 1500s was used to acquire four scans with a spin−echo pulse sequence. For the Li^+-sorbed lepidocrocite, a spin−echo pulse sequence with a pulse delay of 0.15 s and 352000 scans was used. In order to correct the intensities for signal loss during the spin−echo sequence, an estimate for the transverse relaxation (T_2) time was obtained by acquiring four spectra with different evolution/refocusing times.

3. Results and Discussion

3.1. Powder X-ray Diffraction (XRD), Scanning Electron Microscopy (SEM), Point of Zero Charge (PZC), BET Surface Area, Thermogravimetric Analysis (TGA) and Differential Thermal Analysis (DTA) of Lepidocrocite. No significant differences are seen between the XRD powder patterns of γ-FeOOH and γ-FeOOD (Figure 2), and both the positions and relative intensities of the reflections are consistent with those found in the JCPDS file. On the basis of the Scherer and Warren formula,[27] the particle sizes, determined using the more intense reflections, were calculated to be approximately 12 nm. Goethite is observed as a minor impurity phase, the intensities of the reflections due to this phase increasing slightly following the deuteration process. The XRD patterns for the ^7Li-sorbed lepidocrocites obtained as a function of the pH (4.0, 8.1, and 11.4) are identical to those of the starting material (Supporting Information Figure S1), respectively, indicating that lithium adsorption does not affect the structure of lepidocrocite.

(26) Weckler, B.; Lutz, H. D. *Eur. J. Solid State Inorg. Chem.* **1998**, *35*, 531−544.

(27) West, A. R. *Solid state chemistry and its applications;* WSE Wiley: New York, 1998.

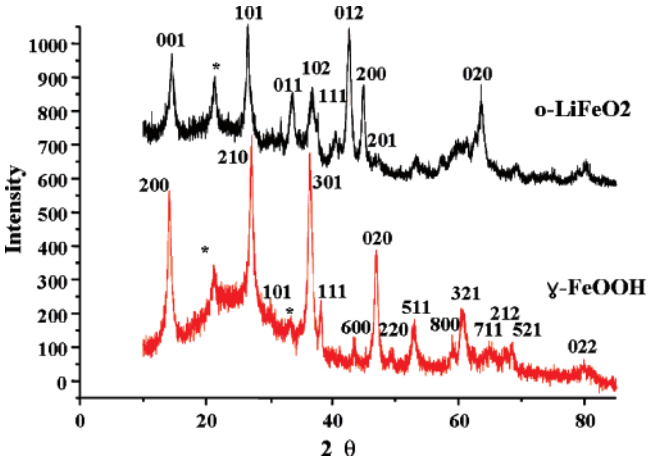

Figure 3. X-ray powder diffraction for γ-FeOOH (bottom) and Li-intercalated lepidocrocite (top). (*) denotes the goethite impurity.

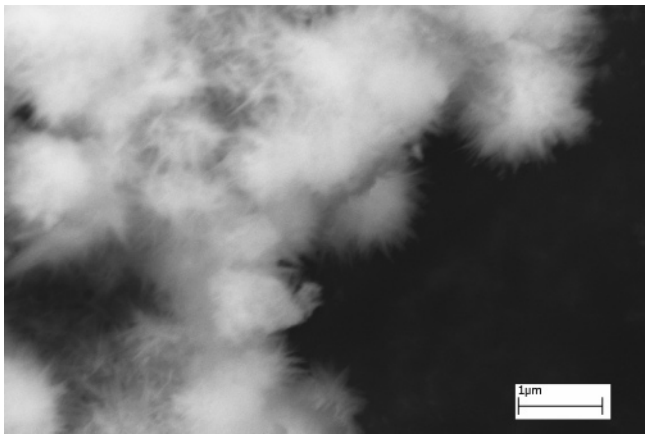

Figure 4. Scanning electron microscopy (SEM) image of lepidocrocite (γ-FeOOH).

In contrast, Li^+ for H^+ ion-exchange results in a noticeable shift of many of the reflections, for example, the low angle reflections near $2\theta = 14°$ (200) and 27° (210) moving to higher and lower angles, respectively, consistent with earlier reports that the *a*-lattice parameter increased while the *b*- and *c*-parameters decreased following the ion-exchange (Figure 3).[22] Therefore, the XRD data indicate that no substantial Li^+ for H^+ ion-exchange has occurred in the Li^+ sorbed samples, suggesting that the Li^+ ions are only adsorbed on the surface. Again, the goethite reflections became slightly more intense following Li^+ sorption, particularly for the high pH sample, consistent with some conversion of the metastable lepidocrocite phase to goethite, during the sorption process.

Examination of the SEM (Figure 4) shows that the lepidocrocite consists of fibrous particles with diameters and lengths of 2 and 300 nm, respectively, that form aggregates of 0.5−1 μm in diameter. This is one of the characteristic morphologies formed by lepidocrocite. Lath-shaped particles comprise the second most common particle morphology adopted by both natural and synthetic lepidocrocites, with the flat (010) surface representing the predominant surface.[19] The morphology adopted by lepidocrocite depends on the conditions used during the synthesis to oxidize the Fe^{2+}, slow oxidation preferentially inducing the lath shapes.[19] Fibrous aggregates, as observed in this study, are formed from very fast oxidation at low pH. The presence of these fibers results in a decrease of the relative ratio

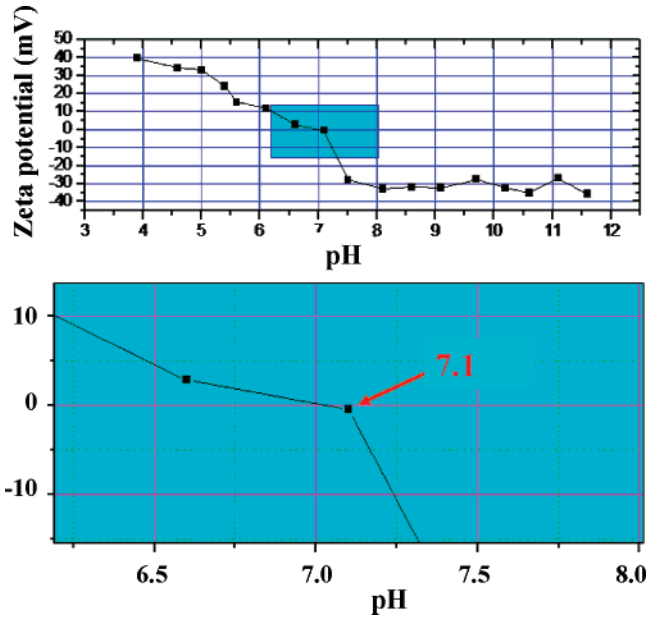

Figure 5. PZC (point of zero charge) analysis curve of γ-FeOOH. The highlighted region in the top curve is expanded in the bottom plot.

of the (010) surface to the total surface area. Nonetheless, this surface still remains the predominant face.[4,28]

Figure 5 shows the PZC measurement for γ-FeOOH. A PZC value close to neutral pH of pH 7.1 ($\pm$0.1) was determined from this data, which is consistent with the previously reported PZC data of 6.7, 7.29, and 7.45.[29−31] This result provides additional support for the predominance of the (010) surface, because the (010) face contains neutral and inert Fe_2OH groups. A BET surface area of 85 m^2/g was measured, which is consistent with previously reported values for materials synthesized by using similar methods.[19]

TGA and DTA experiments were performed to measure the water content and thermal stability of γ-FeOOH. TGA of γ-FeOOH showed a gradual weight loss of 7.5 wt % (Figure 6) from room temperature to 200 °C. This weight loss is assigned to the loss of surface water. On further heating, lepidocrocite showed a much more sudden additional weight loss of 9.5 wt %, indicating the formation of maghemite (γ-Fe_2O_3) via the reaction: 2 γ-FeOOH $\rightarrow$ γ-$Fe_2O_3 + H_2O$. When the temperature approached 400 °C, an endothermic peak was seen in the DTA curve, resulting from the transformation to the more stable hematite (α-Fe_2O_3) phase; a small weight loss accompanies this process, consistent with previous reports,[32] possibly due to loss of residual proton defects in γ-Fe_2O_3. These measurements allowed us to determine the temperature range over which lepidocrocite is stable and thus the range that this material could be studied in our VT NMR experiments.

3.2 Solid-State NMR. 3.2.1. ^{2}H NMR of γ-FeOOD. One local environment was detected by ^{2}H MAS NMR in the spectrum of γ-FeOOD, which gave rise to an isotropic peak centered at about 170 ppm with a large sideband manifold

(28) Sudakar, C.; Subbanna, G. N.; Kutty, T. R. N. *J. Phys. Chem. Solids* **2003**, *64*, 2337−2349.
(29) Gupta, S. K. Ph.D. Thesis. University of Bern, 1976.
(30) Waite, T. D.; Morel, F. M. M. *J. Colloid Interface Sci.* **1984**, *102*, 121−137.
(31) Zhang, Y.; Charlet, L.; Schindler, P. W. *Colloids Surf.* **1992**, *63*, 259−268.
(32) Gehring, A. U.; Hofmeister, A. M. *Clays Clay Miner.* **1994**, *42*, 409−415.

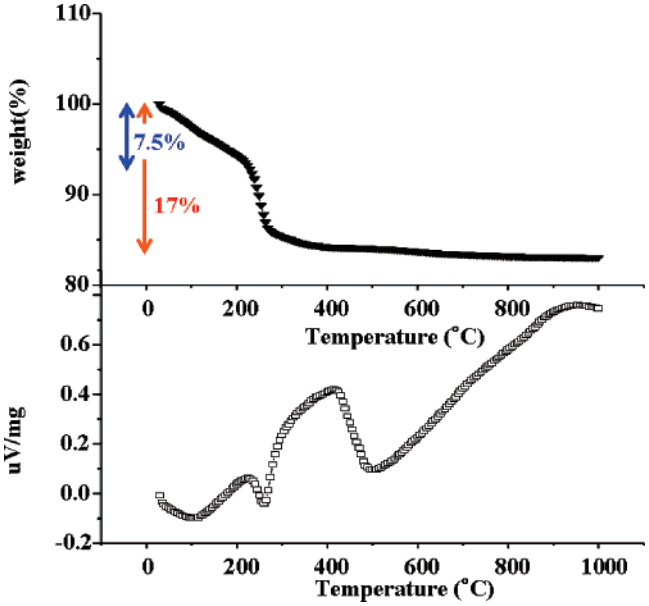

Figure 6. TGA and DTA curves for lepidocrocite (γ-FeOOH).

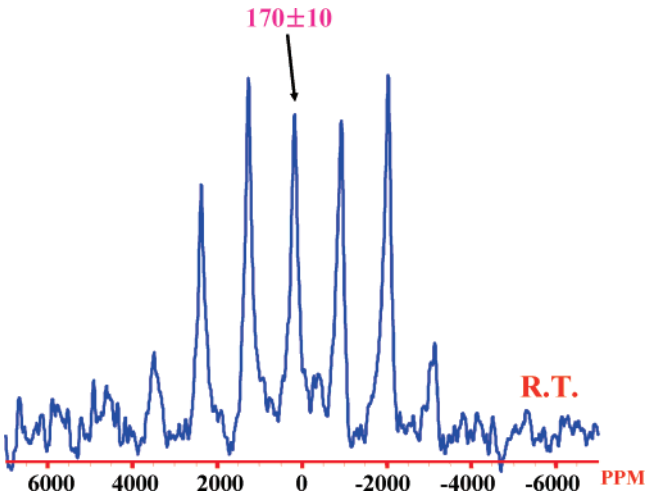

Figure 7. ^{2}H MAS NMR spectrum of γ-FeOOD, acquired at room temperature with a 34 kHz spinning rate at a Larmor frequency of 30.66 MHz. The isotropic resonance is labeled.

(Figure 7). This resonance is assigned to bulk sites on the (010) planes, in between the $[FeO_2]^-$ zigzag layers. A quadrupolar coupling constant (C_Q) of 180(15) kHz was extracted from the ^{2}H MAS NMR spectrum. The C_Q can be used to calculate an O−O distance of 2.65(5) Å, by using eq 1:

$$C_Q\,(\text{kHz}) = 442.7 - 4882/R^3 \qquad (1)$$

where R represents the O−O distance in Å.[17,33] This value is close to the value of 2.676(4) Å previously reported for the bulk structure,[20] confirming the assignment. The envelope of the ^{2}H NMR sideband manifold resembles that of a typical Pake-doublet, indicating that the hydroxyl groups in the structure are rigidly bound between the layers. The large isotropic shift is ascribed to a hyperfine or Fermi-contact shift interaction due to the unpaired spin density that is transferred from the unpaired

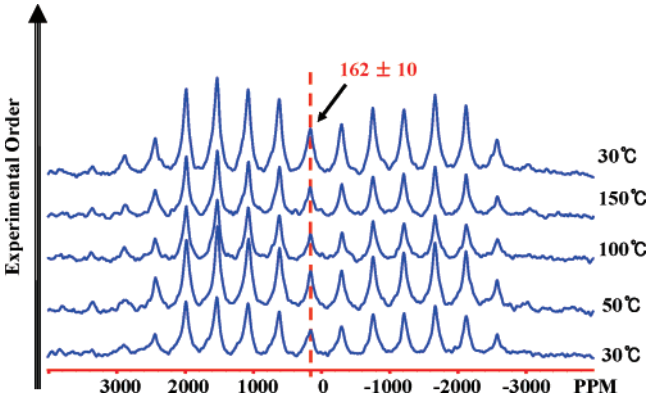

Figure 8. VT ^{2}H MAS NMR spectra of γ-FeOOD at 30, 50, 100, 150, and then 30 °C at a Larmor frequency of 55.27 MHz (from bottom to top). The isotropic resonance is labeled with its hyperfine shift. A MAS spinning speed of 14 kHz was used.

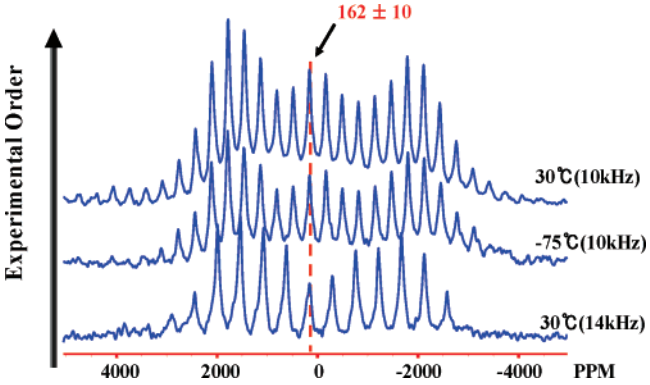

Figure 9. VT ^{2}H MAS NMR spectra of γ-FeOOD at 30 °C (14 kHz), −75 °C (10 kHz), and then on returning to 30 °C (10 kHz) at a Larmor frequency of 55.27 MHz. The isotropic resonances are labeled.

electrons of the paramagnetic Fe^{3+} ions to the empty 1s orbitals of the deuterium atoms. The signals due to the surface OD groups are presumably hidden by the much more intense resonance from the bulk environments. The linewidths of the individual peaks are broader (approximately 3.5 kHz, full width at half-height, fwhh) than those seen for ^{2}H NMR spectra of various MnOOD polymorphs (0.3−1.7 kHz).[34] This is tentatively ascribed, at least in part, to the longer electronic relaxation times of the Fe^{3+}, d^5, unpaired electron spins.

No shift of the isotropic resonance was observed in the VT ^{2}H NMR spectra of γ-FeOOD (Figure 8) on heating up to 150 °C. This behavior deviates significantly from the Curie−Weiss law, which predicts a $1/T$ dependence of the shift, but is consistent with the reported magnetic susceptibility (χ) data reported by Gehring et al.[32] where no significant change in χ was observed in the temperature range studied in this paper. A second set of VT ^{2}H NMR experiments was performed at 30, −75, and 30 °C (Figure 9), and again no significant temperature dependence was observed. Furthermore, no change was observed in the NMR spectra after these VT experiments, indicating that the local environments are unaffected by the temperature treatments. The VT NMR spectra are consistent with the presence of short-range, strong antiferromagnetic (AF) couplings between Fe^{3+} ions at ambient temperature (i.e., well above the Néel temperature, 77 K for lepidocrocite).[4]

(33) Poplett, I. J. F.; Smith, J. A. S. *J. Chem. Soc., Faraday Trans. 2* **1978**, *74*, 1077−1087.

(34) Paik, Y.; Osegovic, J. P.; Wang, F.; Bowden, W.; Grey, C. P. *J. Am. Chem. Soc.* **2001**, *123*, 9367−9377.

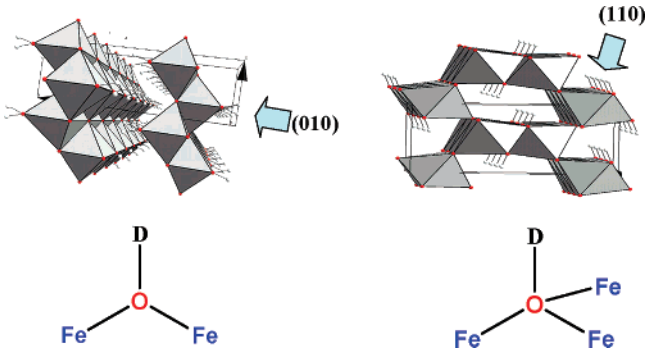

Figure 10. Coordination environments of $^2H^+$ ions in lepidocrocite and goethite. Arrows indicate the major faces.

3.2.2. Comparison of the ^{2}H Hyperfine Shifts Seen for Goethite and Lepidocrocite: The effect of Local Environment vs χ. The size of the hyperfine (or Fermi-contact) shift, H_{cs} is directly proportional to two terms, the time-averaged value of the magnetic moment of the paramagnetic ion,[25] $\bar{\mu}_e$, (which is proportional to the molar susceptibility of the material, χ_M) and the hyperfine coupling constant, A:

$$H_{cs} = -A\frac{B_0}{\mu_0 g N_0 \mu_B}\chi_M \qquad (1)$$

where B_0 is the field strength, μ_0 permeability, g the electron g factor, N_0 Avogadro's number, and μ_B the Bohr magneton. χ_M depends on the number of unpaired electrons and the nature of any residual couplings between magnetic ions in the paramagnetic state, while the size of A is determined by the number of H−O−Fe (or Li−O−Fe) bonds and nature of the overlap between the H (Li) s, O 2s and 2p, and the Fe 3d (and 4s, 4p) orbitals that contribute to these bonds. In order to explore the effect of χ_M on the hyperfine shifts, we now compare the ^{2}H MAS NMR spectra of the FeOOH polymorphs, lepidocrocite and goethite. (The goethite data was previously published in refs 17,18). The ^{2}H NMR hyperfine shifts for OD groups in lepidocrocite are noticeably larger than those in goethite (170 vs 90−140 ppm, respectively, where 90 ppm is obtained for the microsized goethite, and 140 ppm for the nanoparticles), even though the OH groups in goethite are coordinated to three Fe^{3+} ions (Figure 10). NMR experiments were performed for the lepidocrocite and nanosized goethite at 300 K and for the microsized goethite at 400 K (i.e., above its Néel transition).[17,18] The smaller shift of goethite can, however, be rationalized if the differences in χ_M are considered.

The value for χ_M (110×10^{-6} emu/g·Oe)[35] for lepidocrocite at 300 K is approximately 2.75 and 4 times larger than those of nanosized at 300 K and bulk goethite at 400 K, respectively, which are 40×10^{-6} emu/g·Oe[35] and 25×10^{-6} emu/g·Oe,[36] respectively (Table 1). Thus, based on the lepidocrocite shift of 170 ppm, a shift of $170 \times 3/2 \times (40/110)$, i.e., 93 ppm is calculated for nanosized goethite, where we have accounted for both the larger number of H−O−Fe connectivities for goethite (3 vs 2), and the susceptibility. For bulk goethite, a smaller shift of 58 ppm ($170 \times 3/2 \times (25/110)$ ppm) is calculated, consistent with the smaller experimental value seen for this sample (90 ppm). The differences between experimental and calculated values are at least in part ascribed to the noticeable variations in χ_M measured for nominally similar samples. This result suggests that a similar correction will be required when comparing the Li shifts for Li sorption on the goethite and lepidocrocite materials. A second correction may also be required to account for the strength of the O−D bonds (and thus the extent of the H, 1s − O, 2p overlap) for different types of Fe_nO−D groups. Stronger OD groups will be formed in lepidocrocite (containing Fe_2OD groups) than in goethite (Fe_3-OD), which should also lead to larger values of A, and thus hyperfine shifts for lepidocrocite.

Table 1. Comparison of Magnetic Susceptibilities and NMR Shifts[a] (^{6,7}Li and ^{2}H) of Goethite and Lepidocrocite

	χ_M (emu/g·Oe)[35,36]	ppm (^{2}H)	ppm (^{6,7}Li)
γ-FeOOH	110×10^{-6}	170(10)	60
α-FeOOH (micro)	25×10^{-6}	90[17]	
α-FeOOH (nano)	40×10^{-6}	140[18]	140[18]

[a] NMR[17,18] and susceptibilities[35,36] were extracted from data collected at 300 K (γ-FeOOH and α-FeOOH (nanosized)) and 400 K (micron-sized). Li data are those obtained for sorption at pH 11.4.

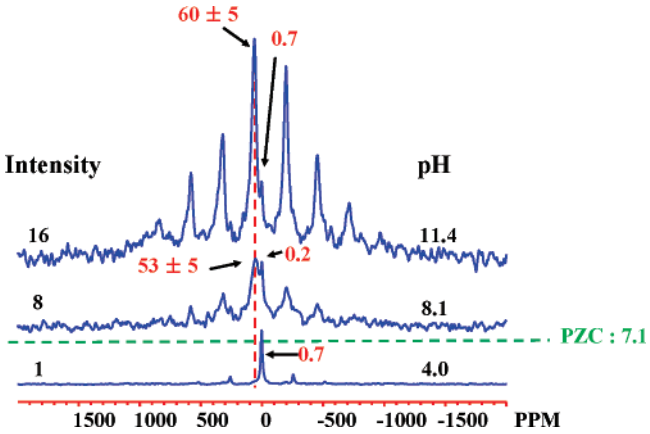

Figure 11. ^{7}Li MAS NMR spectra of lithium-ion sorbed lepidocrocite as a function of the pH, collected at a spinning rate of 20 kHz at a Larmor frequency of 77.76 MHz. The integrated intensities of the higher-frequency (53−60 ppm) resonance (normalized to the intensity of the resonance of the pH 4.0 sample) and the pH of the solutions, are shown on the left- and right-hand sides, respectively.

3.2.3. ^{7}Li NMR of Lepidocrocite. Lithium cation sorption on lepidocrocite was examined by solid-state ^{7}Li MAS NMR spectroscopy as a function of pH (Figure 11). Two main ^{7}Li resonances were observed with isotropic shifts of about 53−60 and 0 ppm, where the positions of these isotropic resonances were confirmed by performing experiments at different spinning speeds of 18 and 20 kHz. As the pH is increased from 4.0 to 8.1 to 11.4, the relative intensity of the higher-frequency resonance increased noticeably (by a factor of 16 from pH 4.0 to 11.4), and the resonance position shifted from 53 to 60 ppm. This indicates that more lithium cations are bound more strongly to the surface of lepidocrocite above its PZC, pH 7.1, than at lower pH. In contrast, no significant change in the intensity of the resonance at 0 ppm was observed as a function of pH. The 53−60 and 0 ppm peaks are assigned to inner-sphere and outer-sphere complexes on the lepidocrocite surface, respectively, on the basis of three main reasons. First, the large shifts of the 53−60 ppm resonances are ascribed to the Fermi-contact shift

(35) Lee, G. H.; Kim, S. H.; Choi, B. J.; Huh, S. H. *J. Korean Phys. Soc.* **2004**, *45*, 1019−1024.
(36) Ozdemir, O.; Dunlop, D. J. *Geophys. Res. Lett.* **1996**, *23*, 921−924.

mechanism in which the unpaired spin density due to the Fe^{3+} ions is partially transferred to the empty 2s orbitals of the Li^+ ions through direct Fe−O−Li bonds. A large hyperfine shift is not predicted for the resonance of the outer-sphere complex since it has no direct Li−O−Fe bonds (i.e., the Li^+ ion has no Fe^{3+} ions in the cation first-coordination shell). Second, the intensity of the resonance assigned to the inner-sphere complex is much more sensitive to the pH changes than the intensity of the resonance assigned to the outer-sphere complex. Third, the spectrum of the low loading sample prepared with a 10 mM LiOH solution (not shown here) also contained a resonance with the same large hyperfine shift as that seen for samples prepared with a 50 mM LiOH concentration solution. This allows us to rule out the possibility that the 53−60 ppm resonance is due to the formation of a Fe^{3+}-containing precipitate. An the adsorption density for the inner-sphere complex at pH 11.4 was calculated on the basis of the signal intensity of the inner-sphere resonance obtained in the ^{7}Li MAS NMR spin-counting experiments and the BET surface area of 85 m^2/g. The intensity of the signal was corrected for the short T_2 (approximately 0.2 ms), of the inner-sphere resonance, which leads to approximately 29% of signal loss during the two rotor periods (approximately 0.11 ms) of the spin−echo experiment, resulting in a corrected adsorption density of 3.1 × 3.1 nm^2 per Li ion (i.e., one Li^+ occupies, on average, a surface area of 9.6 nm^2 or 0.1 Li^+/nm^2). [N.b., the short T_2 of this resonance is not due to the short spin−lattice relaxation time (T_1) for Li^+ in this environment, since a T_1 value of 5.0 ms was measured, and further experiments are in progress to identify some of the causes of the short T_2. We note, however, that it is not due to broadening due to the anisotropic bulk magnetic susceptibility.[37]]

The resonance at ~0 ppm is assigned to a Li^+ outer-sphere complex. To confirm this assignment and to ensure that the resonance does not arise from only diamagnetic impurities such as lithium carbonate (Li_2CO_3) or lithium bicarbonate ($LiHCO_3$), due to incomplete ion exchange or washing, a series of relative humidity (RH) experiments was performed. These experiments were also performed so as to explore the effect of RH on the relative concentrations of the inner- and outer-sphere complexes (Figure 12). The intensity of the 0 ppm peak increased as a function of increasing relative humidity (0, 30, and 84% RH). An even larger change was seen between the ^{7}Li MAS NMR spectrum of the wet paste and the dried sample (Figure 13), the ratio of the 60 to 0 ppm peak intensity decreasing from approximately 6 to 1 on hydration, as determined by peak integration. This was associated with a decrease in the absolute intensity of the 60 ppm resonance by a factor of 2. The increase of the peak intensity of the 0 ppm resonance is ascribed to the increased hydration of the Li^+ inner-sphere complexes, and the formation of outer-sphere complexes (Figure 14). This result confirms that the 0 ppm resonance is due to an outer-sphere complex and not solely a diamagnetic impurity or precipitate on the particle.

3.2.4. Assigning the Li Hyperfine Shifts to Specific Surface Sites: A ^{6,7}Li NMR Investigation of a Model Iron (III) Oxide. The size of the Fermi-contact shift (i.e., hyperfine) interaction is strongly dependent on the number of Li−O−Fe bonds. Thus, to assign the ^{7}Li NMR resonance at 60 ppm to specific surface site(s), we synthesized the Li-intercalated layered compound

(37) Alla, M.; Lippmaa, E. *Chem. Phys. Lett* **1982**, *87*, 30−33.

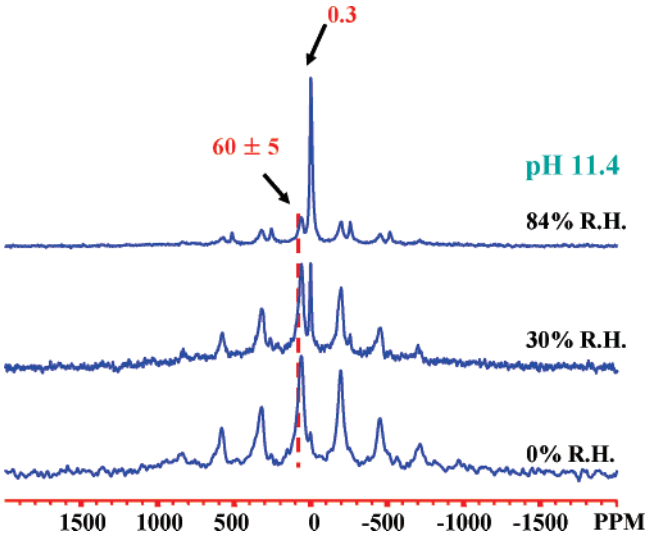

Figure 12. Effect of relative humidity on the ^{7}Li MAS NMR spectra of lithium-sorbed lepidocrocite at pH 11.4, collected at a spinning rate of 20 kHz at a Larmor frequency of 77.76 MHz.

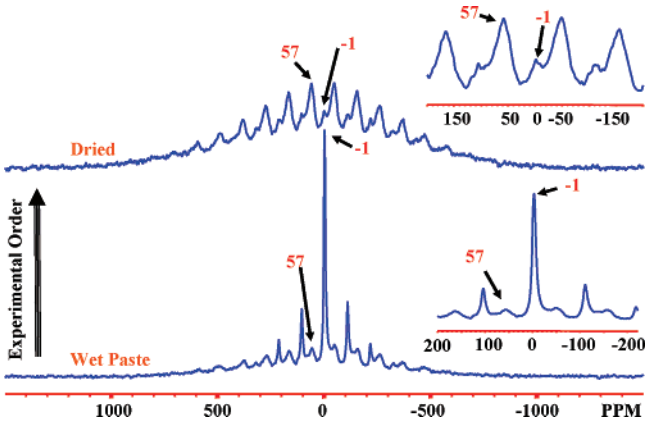

Figure 13. ^{7}Li MAS NMR spectra of the wet paste and the dried sample of Li^+ sorbed on lepidocrocite at pH 11.4, collected at a spinning rate of 15 kHz at a Larmor frequency of 140 MHz.

o-$LiFeO_2$, which is derived from lepidocrocite via Li^+ for H^+ ion-exchange. In principle, this material should serve as a model compound to allow us to estimate the contribution per Li−O−Fe(III) bond to the overall hyperfine shift, because the position of Li^+ in this material is well characterized.[22,23] The ^{7}Li MAS NMR spectrum of *o*-$LiFeO_2$ contains one resonance with an isotropic resonance of about 317 ppm, which is assigned to Li^+ in an octahedral site between the layers (Figure 15). The resonance at −1.8 ppm is assigned to diamagnetic impurities such as Li_2CO_3 or $LiHCO_3$ due to its small chemical shift. This result additionally confirms that the resonance at 60 ppm, seen in the Li^+-sorbed samples, is not due to Li^+ ion-exchanged in between the lepidocrocite layers.

Li^+ in the octahedral site between the $[FeO_2]^+$ layers of *o*-$LiFeO_2$, contains six Fe^{3+} ions in its first cation coordination shell which are connected to Li^+ via 12 Li−O−Fe^{3+} bonds with bond angles of approximately 90°.[22,38] Four Fe^{3+} ions are located in the second cation coordination shell resulting in four Li−O−Fe bonds, with bond angles of approximately 180° (Figure

(38) Kanno, R.; Shirane, T.; Inada, Y.; Kawamoto, Y. *J. Power Sources* **1997**, *68*, 145−152.

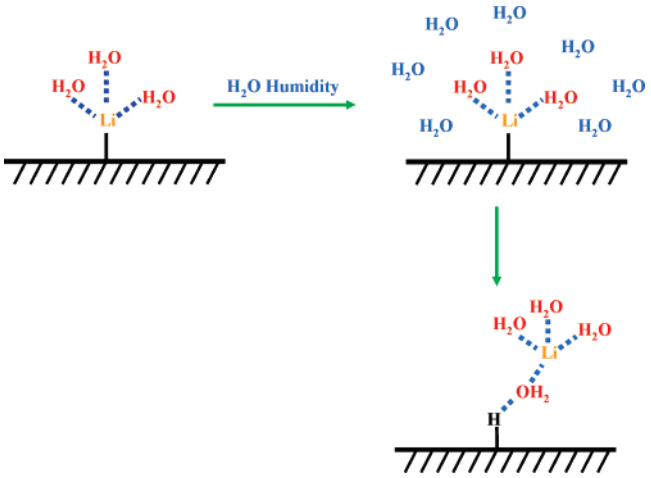

Figure 14. Schematic showing the effect of humidity on Li^+ binding to the lepidocrocite surface.

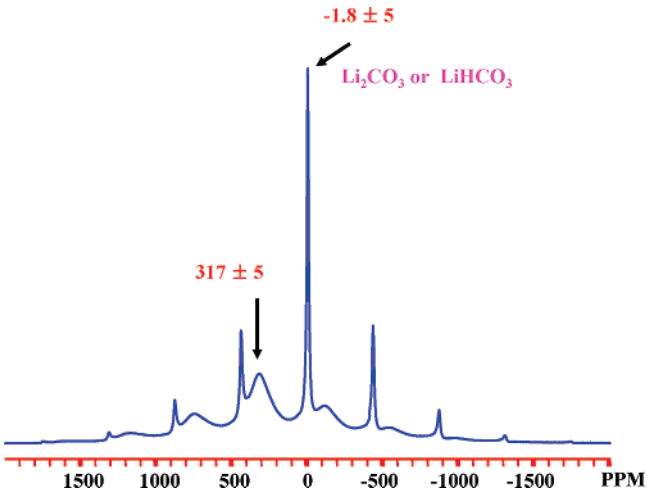

Figure 15. ^{7}Li MAS NMR spectrum of lithium-intercalated *o*-LiFeO2, collected at a spinning rate of 37 kHz at 77.76 MHz.

16), forming a total of 16 Li−O−Fe connectivities. If the surface-bound Li^+ was located in the same octahedral site, but now on the (010) surface, then the Li^+ ion is connected to 7 Fe^{3+} ions via 10 Li−O−Fe 90° bonds and two 180° bonds. Given that this environment contains more than half the total number of Li−O−Fe connectivities of the octahedral Li site in *o*-$LiFeO_2$, and thus should be associated with a shift of greater than (317/2 =) 159.5 ppm, it is immediately clear that the 60 ppm resonance cannot be assigned to this environment. Thus, a more detailed analysis of the hyperfine shift mechanism is required.

As discussed above for the ^{2}H spectra, the size of the hyperfine shift will depend on the number and nature of Li−O−Fe bonds and the molar susceptibility of the material, χ_M. We assume that χ_M is very similar for lepidocrocite bulk and surface sites which, given the nature of the termination of the surface, appears reasonable (Figure 1), but this is an assumption that will require testing in future studies. On the basis of our previous investigations of Li^+ hyperfine shifts and the high-spin electronic configuration for Fe^{3+} of $t_{2g}^3e_g^2$, both Li−O−Fe 90° and 180° interactions will result in positive contributions to the hyperfine shift, the former via an interaction between the t_{2g} half-filled d orbitals and the adjacent 2p O orbitals, and the latter via an e_g (Fe) and 2p (O) interactions. At this point, it is difficult to determine the relative importance of each contribution, but we note that 90° interactions involving half-filled t_{2g} orbitals in Li−O−Mn^{4+} bonds give rise to similar sizes of shifts as Li−O−Ni^{2+} 180° interactions involving half-filled e_g orbitals.[25,39] Thus, as a first approximation, we assume that they result in similar contributions to the overall hyperfine shift. Given a hyperfine shift of 317 ppm for the Li^+ ions in the octahedral site of *o*-$LiFeO_2$, a contribution to the hyperfine shift of 20−22 ppm per Li−O−Fe connectivity can be estimated. This estimate is slightly lower than that obtained on the basis of the ^{6}Li NMR shifts observed for the α- and γ-$LiFeO_2$ polymorphs. These materials contain a total of 20 Li−O−Fe bonds in the first and second cation coordination shells, and ^{6}Li shifts that range from 471 to 543 ppm,[40] giving rise to an average shift of 23−27 ppm per Li−O−Fe bond. Differences between the shifts calculated for the two sets of compounds presumably arise from variations in χ, Li−O−Fe bond angles and the degree of Li−O and Fe−O overlap. At this point, it seems reasonable to assume a lower limit of 20 ppm for a Li−O−Fe bond and an upper limit of 30 ppm for compounds (and local environments) with similar values of χ_M.

3.2.5. Locating the Li^+ Positions on the Surface of Lepidocrocite. The lepidocrocite surface is dominated by three faces, (010) (major), and (100), and {001} (minor).[4,41,42] The major (010) face is terminated via inert Fe_2OH groups, which are not readily deprotonated. Both the {001} and (100) faces of lepidocrocite have two reactive (proton-terminated) sites, FeO and Fe_3O.[41] On the basis of a semiempirical model (the MUSIC model), which assigns to partial charges to the various O sites, according to bond valence sums calculated from the number and lengths of the Fe−O bonds and coordination environments of the Fe and O ions,[4,41] the pK_a's for the two groups are predicted to (i) be different for the two surfaces, and (ii) depend quite sensitively on H-bonding to other nearby oxygen atoms, complicating the analysis. The FeOH groups are expected to be only present at high pH, whereas $FeOH_2$ groups will be formed at neutral pH; the $FeOH_2$ groups are more readily deprotonated than the Fe_3OH groups. The {001} face can be further subdivided into the (001) and (00$\bar{1}$) faces. The PZC of the (001) face is predicted to be lower than that of the (00$\bar{1}$) face, again according to the MUSIC model.[41]

The shift of 20−30 ppm per Li−O−Fe connectivity, estimated on the basis of the model compounds, suggests that Li^+ ions on the lepidocrocite surface should be coordinated to oxygen atoms in the $[FeO_2]^-$ sheets that are bound to a total of no more than two or three Fe^{3+} ions (Table 2). Based on this hypothesis, six possible surface adsorption sites (A1−A6) for Li^+ among the many potential adsorption sites can be identified (Figure 17). These can then be further reduced to a binuclear bidentate (A4) and a monodentate complex (A6), based on the following reasons. The edge-sharing bidentate complexes, A2 and A5, are excluded because there are no known edge-sharing

(39) Carlier, D.; Menetrier, M.; Grey, C. P.; Delmas, C.; Ceder, G. *Phys. Rev. B: Condens. Mater. Phys.* **2003**, *67*, 174103.
(40) Pan, C. Li NMR Studies of $LiMO_2$. M. Sc. Thesis. SUNY, Stony Brook, New York, 2000.
(41) Venema, P.; Hiemstra, T.; Weidler, P. G.; van Riemsdijk, W. H. *J. Colloid Interface Sci.* **1998**, *198*, 282−295.
(42) Randall, S. R.; Sherman, D. M.; Ragnarsdottir, K. V.; Collins, C. R. *Geochim. Cosmochim. Acta* **1999**, *63*, 2971−2987.

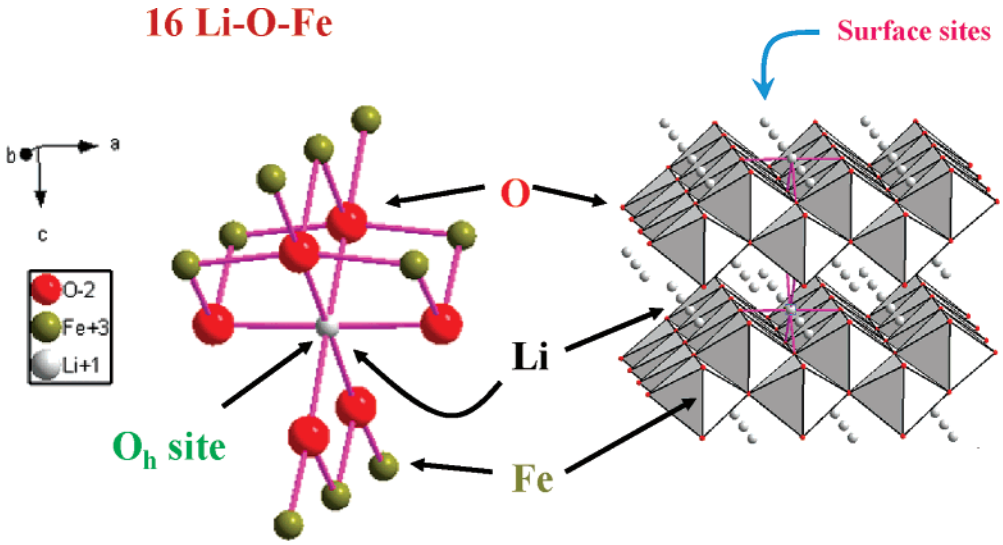

Figure 16. Structure of *o*-$LiFeO_2$ showing the local coordination environment for Li^+ (left-hand side).

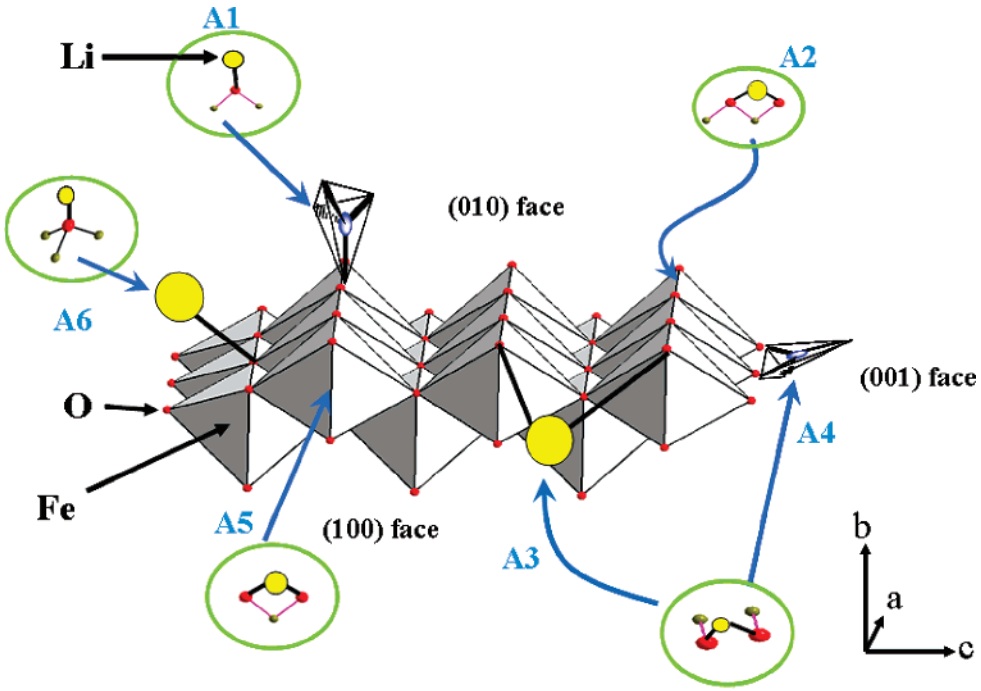

Figure 17. Possible positions for the lithium cations on the surface of lepidocrocite.

Table 2. Calculated Hyperfine Shifts for Different Possible Sites for Li^+ Adsorption

sites	number of Li–O–Fe bonds	NMR shift (ppm)
A1	2	40−60
A2	3	60−90
A3	2	40−60
A4	2	40−60
A5	2	40−60
A6	3	60−90

structures involving $Fe^{3+}O_6$ octahedral and tetrahedral oxyanions in crystalline solids.[43] The monodentate complex, A1, is less favorable because Fe_2OH groups on (010) faces are expected to be inert and will not be deprotonated at the pH ranges studied here.[4,41] In addition, the monodentate A1 site on the (010) surface is entropically less favorable than the bidentate sites, A3 and A4, because of the chelate effect.[43] The monodentate Fe_3O (A6) site is located on the $(00\bar{1})$ face. Since it can only be deprotonated at high pHs it will likely only contribute to the 60 ppm resonance observed in the pH 11 spectrum. The O−O distances for the double corner-sharing binuclear A3 and A4 complexes on the {001} and (100) faces, respectively, are very different, the two faces having (unrelaxed) O−O distances of 3.07 and 3.88 Å, respectively, based on the distances of the bulk material.[20] Given a typical Li−O distance of about 1.7 to 2 Å, (the exact value depending on the Li coordination number) the O−O (A3) distance on the (100) face is too long for a Li^+ ion to bind simultaneously to both oxygen atoms, unless a close-

(43) Sherman, D. M.; Randall, S. R. *Geochim. Cosmochim. Acta* **2003**, *67*, 4223−4230.

to-linear O−Li−O linkage is formed. In this case, there will also be a very short contact with a third oxygen atom (coordinated to three Fe^{3+} ions), and much larger hyperfine shifts are predicted. Consequently, we propose that only the A4 site on the {001} faces plays a major role in adsorbing Li^+ at pH 8 and higher, via the formation of corner-sharing binuclear complexes involving the FeOH binding sites. This site must remain a major sorption site until pH 11, because there is only one major local environment for Li^+ from pH 8.1 to 11.4 in our ^{7}Li NMR spectra (Figure 11). The increase in intensity of the ^{7}Li resonance from pH 8.1 to 11.4 is consistent with the increased deprotonation of the $FeOH_2$ sites (to form FeOH and thus more basic, under coordinated, oxygen sites), and the availability of additional sites such as the Fe_3O, A6 site. These observations are consistent with our measurement of a very low loading level for Li^+ on the surface of lepidocrocite (0.1 Li^+/nm^2) based on the spin-counting experiments, since all these sites lie on the minority (001)/(00$\bar{1}$) faces.

Our model for Li^+ adsorption on lepidocrocite is similar to models suggested for binding of other small ions such as Cu^{2+} and Cd^{2+}, which have also been proposed to form bidentate corner-sharing complexes on the {001} face.[12,13] However, Cd^{2+} also forms an edge-sharing complex on the octahedral site of the [010] surface. We do not see any evidence for Li^+ binding to this site in our hydrated samples.

Finally, on the basis of our additional NMR data for lepidocrocite we can reanalyze the positions for Li^+ on goethite, taking into account the dependence of the hyperfine shift on the bond connectivities between Li^+ and Fe^{3+}. We previously reported ^{7}Li NMR shifts of 55 and 140 ppm for Li^+ sorbed on goethite at neutral and high pH, respectively, and 289 ppm for Li^+ exchanged inside the tunnels of goethite.[18] The number of binding sites at high pH is noticeably higher than that at close to neutral pH and much higher than the numbers seen for lepidocrocite when the intensity is normalized to both Fe content and surface area. This implies that Li^+ sorbs on a major goethite surface, i.e., the (110) surface, at high pH. The increased hyperfine shift indicates that Li is binding to multiple oxygen ions. Furthermore, the larger shift, 140 ppm, is now half that seen for Li^+ in the tunnels of goethite (289 ppm), suggesting that Li^+ on the surface is coordinated to Fe via approximately hslf the number of Li−O−Fe bonds that are available to the Li^+ ions in the tunnels. The similarity between the hyperfine shift seen in goethite at low pH (55 ppm) and that for lepidocrocite indicates that similar local environments are involved, i.e., bidentate linkages on edges, involving deprotonated $FeOH_2$ groups (Figure 18a). That these $FeOH_2$ groups can be deprotonated at neutral pH is consistent with this statement. At high pH, the Fe_3OH groups will also be deprotonated, leaving a large number of under-coordinated oxygen atoms on the (010) face. A higher coordinate site for Li^+ is now present in the pockets that are formed when the tunnels are sliced to expose the (110) plane (Figure 18b). This site is similar to the site for Li in the tunnels except that binding to only two tunnel walls is now possible. This site will allow binding to more Fe^{3+} ions and is consistent with the large shift seen at high pH.

4. Conclusion

High-resolution NMR spectroscopy of the paramagnetic, iron oxyhydroxide polymorph lepidocrocite has been used to determine hydrogen-bonding distances (^{2}H MAS NMR) and quantify and characterize lithium binding sites (^{7}Li MAS NMR). The large hyperfine shift interactions seen in this system were exploited to distinguish between inner-sphere complex and outer-sphere complexes, and two possible adsorption sites of Li^+ were proposed on the basis of the sizes of the hyperfine shifts. Li^+ forms a bidentate complex on the minor (001)/(00$\bar{1}$) faces (i.e., the edges) of lepidocrocite by binding to two FeOH oxygen atoms at just above the PZC (7.1). At higher pHs, Fe_3-OH sites on the (00$\bar{1}$) face become deprotonated, and the formation of second monodentate complex is also likely. Much lower binding concentrations were seen on lepidocrocite, in comparison to the Li binding concentrations seen in our previous study of goethite.[18] Two binding sites for Li^+ on goethite are proposed, both on the major (110) face. Goethite contains tunnels that run down the [001] direction, and the (110) face is formed by slicing the tunnels, exposing pockets and edge sites, the latter comprising Fe_2OH and FeOH sites. Just above the PZC, Li^+ binds to a bidentate site that is similar to that seen for lepidocrocite, involving two FeOH groups. At pH 11, again the Fe_3OH sites become deprotonated, and a site involving both Fe_3O and FeOH oxygen atoms, in the pockets, is occupied by Li^+.

Iron (oxy)hydroxides are ubiquitous in the environment and major sorption sites for toxic ions and are thus used as cheap sorbents in remediation. The work presented in this paper clearly demonstrates that MAS NMR spectroscopy can used to study ion binding on these classes of materials, opening up new approaches for characterizing and understanding function in these environmentally relevant systems. The approach can be

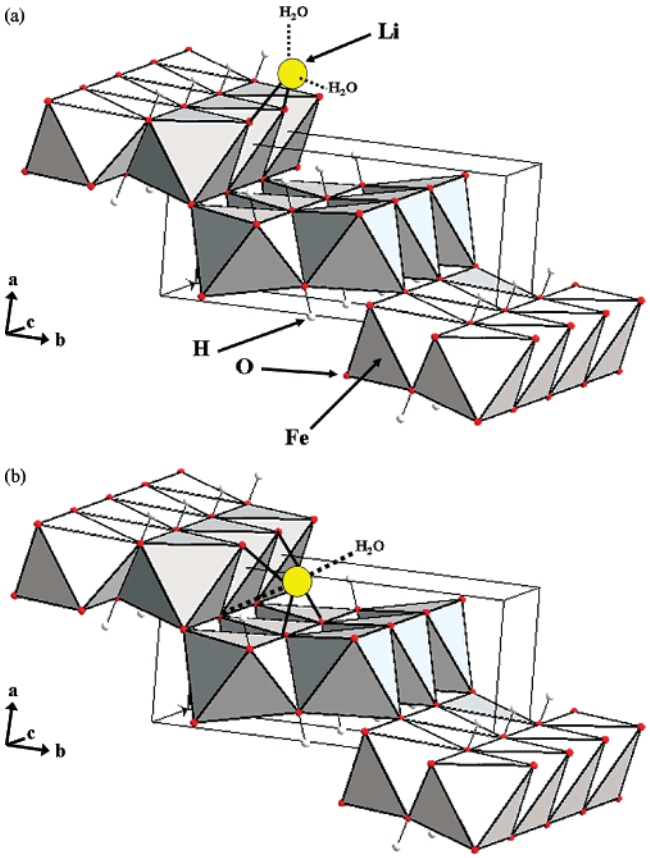

Figure 18. Predicted positions for the lithium cations on the surface of goethite at (a) neutral and (b) high pH.

extended to investigate other paramagnetic systems and to study binding of other, more environmentally relevant sorbents. The water−solid interface represents one of the more poorly characterized systems, particularly in systems where no single crystals are available, yet its structure and dynamics are relevant to the understanding of a wide range of materials and applications, from water splitting catalysts to alkaline batteries. The application of similar NMR approaches to investigate binding in a much wider range of materials can be readily envisaged.

Acknowledgment. The Center for Environmental Molecular Science is funded by the NSF (Grant CHE-0021934). We thank Marc Michael for his help with the PZC measurement in Department of Geosciences, Stony Brook University. We acknowledge Jim Quinn for SEM and Shanshan Liang for TGA and DTA measurements in Materials Science and Engineering Department, Stony Brook University. We thank Natalya Chesnova for helpful discussions. U.G.N. acknowledges the "Camille and Henry Dreyfus Postdoctoral Program in Environmental Chemistry" and Carlsbergfondet (ANS-1323/20) for financial support.

Supporting Information Available: XRD patterns for γ-FeOOH and ^{7}Li-sorbed lepidocrocite at pH 4.06, pH 8.1, and pH 11.4. This material is available free of charge via the Internet at http://pubs.acs.org.

JA0761028